The Lund Observatory Method for IUE Spectral Image Processing

Peter Linde & Dainis Dravins

Lund Observatory, Box 43, S-221 00 Lund, Sweden

1. Introduction

Since 1978 we have used the International Ultraviolet Explorer (IUE) satellite to monitor the solar-type star β Hydri (G2 IV) in order to detect long-term variations in chromospheric activity. The indicators we use are the Mg II h and k emission lines near 280 nm. Since the start of the project more than 90 exposures have been obtained with the IUE LWR camera in high dispersion mode. This represents a unique IUE data collection for a single star.

β Hydri is estimated to be about twice as old as the sun. Current astrophysical theory predicts that this should result in a lowered overall magnetic- and chromospheric activity. This also implies that any variations of the Mg II emission line intensities are expected to be small. Preliminary data reductions, basically using the standard IUE software package (IUESIPS), have shown this to be correct. The variations are usually less than 10-20%. Since the overall precision of the IUESIPS software lies at about 10%, an improvement of the software is essential in order to firmly establish the behaviour of the β Hydri chromospheric activity.

2. IUESIPS shortcomings

During the highly successful IUE project, the IUESIPS software has been enhanced many times. This has resulted in a somewhat heterogeneous treatment of data collected during a period of years, considerably affecting our study. Additionally, it is clear that even the latest IUESIPS version can be improved on several points. This has also been done by several groups. Most of these improvements have been achieved as a result of more advanced spectral data extraction from an input image whose geometrical and

photometric corrections still are made by the IUESIPS software. However, by improving also the way the geometric and photometric corrections are carried out, it is possible to create a corrected image with significantly less noise. These improvements are essentially independent of the extraction improvements, resulting in a final spectrum output of considerably enhanced quality. This is the basis for our software package.

3. Fixed pattern vs. random noise

The data concerning β Hydri available to us give interesting possibilities to study variations in the IUE LWR detector output since 1978. In particular, we have set up a sequence of different raw exposures and displayed them in our image processing system as a time series (movie). It revealed that most of the inter-order background variations are in fact not random but rather display a fixed pattern. The same experiment was repeated for images corrected by IUESIPS. Surprisingly, most of the fixed patterns still remained. Concerning images processed after March 1981 (see below), the effect was even more pronounced, in fact the difference between the raw images and corrected images was small. This suggested that the geometric transformation, and subsequently the photometric calibration, could be improved.

4. An improved image calibration

The problem in the current IUESIPS treatment of the raw images lies in the fact that the geometric transformation made in order to make the raw images register with the pre-exposed flat fields is not sufficiently exact. The reseau marks present in the raw images, intended to be used as reference points for geometric transformation, are considered to be too difficult to detect by an automatic procedure. Instead, indirect information, such as e.g. temperature measurements, is used to compute and apply an approximate geometric transform. However, since the flat fields show strong pixel-to-pixel sensitivity variations on a 10% level, a mismatch of only one pixel results in significant errors in the photometric calibration. We have developed a procedure to obtain a more accurate geometric transformation.

5. Flat field studies

Already in 1980 we obtained from VILSPA the series of 12 flat field exposures that were in use at the time. An initial study of flat field properties was presented at the Vienna IUE Data Analysis Workshop (Dravins and Linde, 1980) Recently, we have obtained the latest available flat field series (LWR ITF2), which are used in the present work.

The flat fields as delivered have been geometrically transformed using the inherent reseau marks as reference points. The reseaus themselves have been removed. A close look at the flat fields shows various irregularities. In addition to the local and global sensitivity variations, a global Moiré-like pattern is present, in the form of streaks of locally lowered pixel-to-pixel variations. We have simulated the process of geometrically

transforming a flat field image. Using the same transform that was applied to the original flat fields, we could generate the same Moiré-type pattern in the transformed output image. We conclude that the smoothed streaks seen in the flat fields (Dravins and Linde, 1980) are simply an effect of the interpolation between pixels needed when making a geometric translation. Obviously, some photometric information is lost in this process.

The adopted IUESIPS procedure until March 1981 was to transform the raw image in order to make it register with the flat fields, and then to apply the photometric calibration. Then the algorithm was changed, and has since been equivalent to a retransformation of the flat fields, making *them* register with the untouched raw images. The rationale behind this was that the spectral resolution would not suffer from a geometric transformation. However, even if the implied geometric transformation was made perfectly, it is clear that such a procedure will further smooth the flat fields, decreasing even more the quality of the photometric content. This explains the observations mentioned in section 3.

It can be shown (i.e. by blinking raw and flat field images), that the fixed pattern seen in the inter-order background of the raw images, is locally identifiable also in the flat field. This proves that the pattern simply is a reflection of varying pixel-to-pixel sensitivity and/or null level. Since this can be done at any desired point in the raw image, we have a *direct* means to obtain information about how to transform the raw image correctly. Thus, within *each* raw image a correlation can locally be made between the raw and flat field images. The method allows close interspacing of the corresponding points in the respective images. The reseau marks, which are present in the raw images, need never be used.

6. Outline of the method

The following are the major items of the current software reduction package:

- selection of a relevant subimage in the raw image and the flat field image
- pattern matching between the raw image and a suitable flat field image
- rearrangement of the corresponding point data in order to obtain a vector field, defined on a square grid, describing the geometric transformation
- geometric transformation of the raw image, combined with an optimised photometric calibration
- magnification of the corrected image
- rotation of the corrected and magnified image to get the spectral orders arranged along a straight axis
- extraction of the background and the spectrum, using optimised slits
- final analysis of the extracted spectrum

6.1 Subimage selection

Since in our project we only need information about the Mg II emission lines, we can restrict our image processing to a limited area of the full IUE image. The Mg II lines appear in two subsequent echelle orders so two subimages are selected. The size has been set to 241*273 pixels. Corresponding subimages are selected in a suitable flat field. The DN (Digital Numbers, DN, are the original image flux units) level of the flat field should correspond to the level of the inter-order background to be used for the pattern matching. For most of our images, this means a combination of the first (lowest exposed) flat field level with the null (no exposure) flat field.

6.2 Pattern matching

A pattern matching procedure is used to find corresponding positions in the raw and flat field images, respectively. First, a *template* (subimage) of size 7*9 pixels is extracted from the raw image. A special algorithm positions the template between the spectral orders in a controlled manner. The template is checked against pixel threshold limits, in order to throw away any remaining pixels that are either too bright (belonging to a spectral order) or too dark (i.e. a reseau mark). Second, a *window* of size 15*17 pixels is extracted from the flat field image. The centre position of the window is precomputed from an approximate global geometric transformation equation. The template is then moved around at all positions in the defined window.

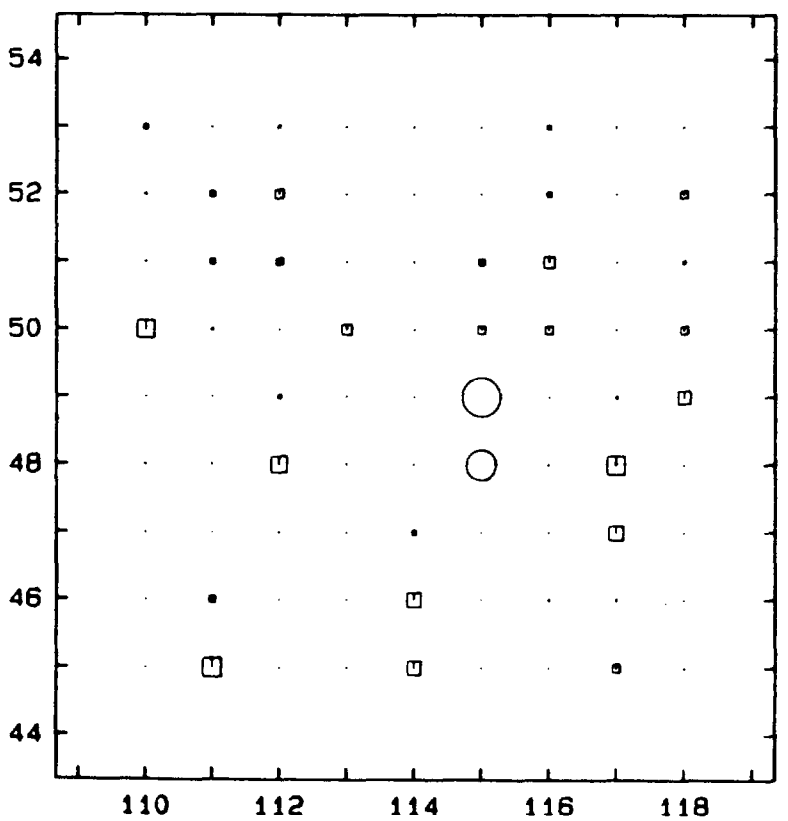

Figure 1. An example of a matrix of normalised correlation coefficients. Each point represents a correlation between the template pixels and the window pixels at that position. The symbol sizes are proportional to the correlation value. The squares are rejected values, while the circles represent accepted values. The axes are denoted with pixel positions in the flat field subimage.

In each position, a normalised correlation coefficient between the template pixels and the window pixels is computed. The result is a matrix of correlation coefficients (see Figure 1). Since it is unlikely that the maximum correlation takes place at an integer coordinate position, the correlation matrix is subject to further analysis. Spurious high correlations are identified and discarded. Among the remaining accepted correlation values, the neighbourhood of the maximum correlation is considered, and a weighted mean is computed. This value defines the position in the flat field image window corresponding to the raw image template position. The procedure then continues with a new template in the raw image, a new window position, a new sequence of correlations, etc. The whole raw image is gone through in a systematic manner, all the time at inter-order positions. Due to the existence of random noise and the partly smoothed flat fields, the correlation values sometimes are too low to allow a safe identification. A threshold level is set on the minimally allowed correlation value. If this level is not reached, the template is systematically displaced a small amount until the correlation becomes satisfactory. Figure 2 shows an example of correlated points, where the size and direction of the vectors define the amount of displacement between the images.

6.3 Computing the transformation vectors

The information from the correlation program consists of a set of corresponding points in the raw and flat field images. Since the template positions can not be defined exactly in advance, the points tend to be irregularly dispersed over the raw image. To perform the geometric transformation, it is necessary to rearrange the information on a regular grid. We have chosen to define a grid with 20 pixels interspacing. An interpolation, using two-dimensional cubic splines for x and y independently, gives the final vector field describing the geometric transformation (see Figure 3). This process also iteratively throws away data which differ more than a threshold value from the interpolated solution. The 20 pixels grid spacing should be compared to the 55 pixels interspacing of the original reseau grid. Our method thus allows for a higher precision correction than the reseau marks would. We have noticed cases where this is significant.

6.4 Transformation and photometric calibration

The photometric calibration is done using the latest available set of flat field images. The flat field data is preprocessed by an interpolation technique involving cubic splines (see Figure 4). For reasons of speed, the spline coefficients are stored and subsequently used by the calibration procedure.

The transformation information derived previously is used to drive the transform algorithm, producing the geometrically corrected image. An unavoidable minor error arises from the fact that the pixel interpolation is done in non-linear DN-space. However, the net effect is that the raw image is corrected (or distorted) the same way as the flat field image previously has been, with the same inherent interpolation smoothed streaks. The photometric calibration for each pixel is then done using the spline data described above.

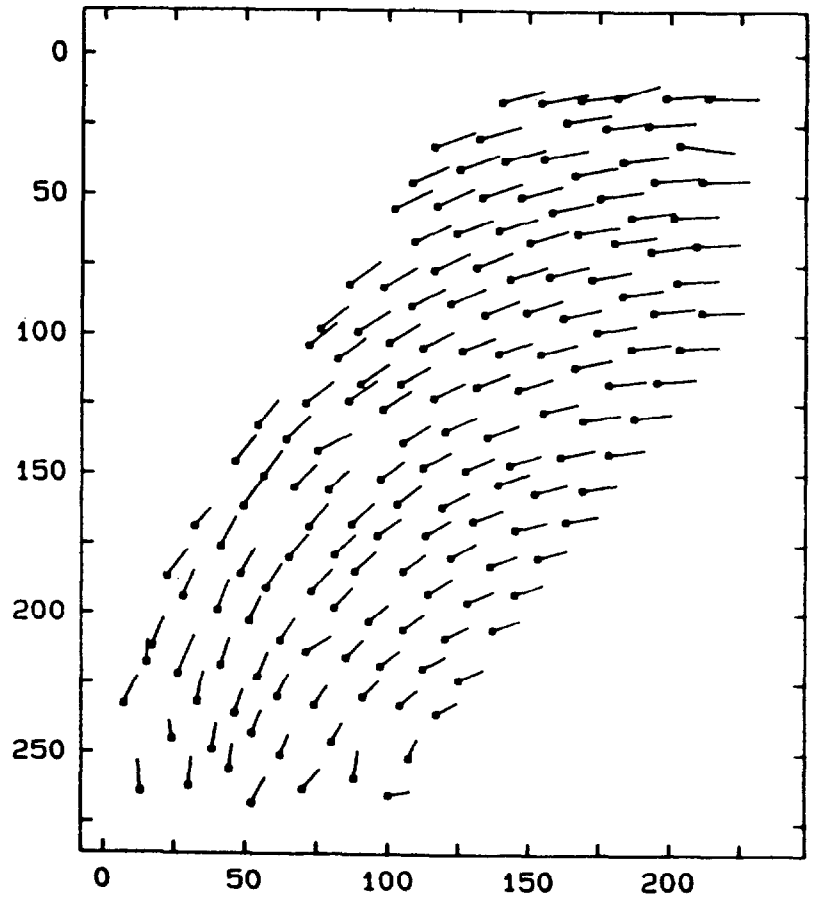

Figure 2. Corresponding point pairs for a subimage of exposure LWR 10605. The points show positions in the raw image and the vectors points to corresponding positions in the flat field. The axes are denoted with pixel positions in the raw subimage.

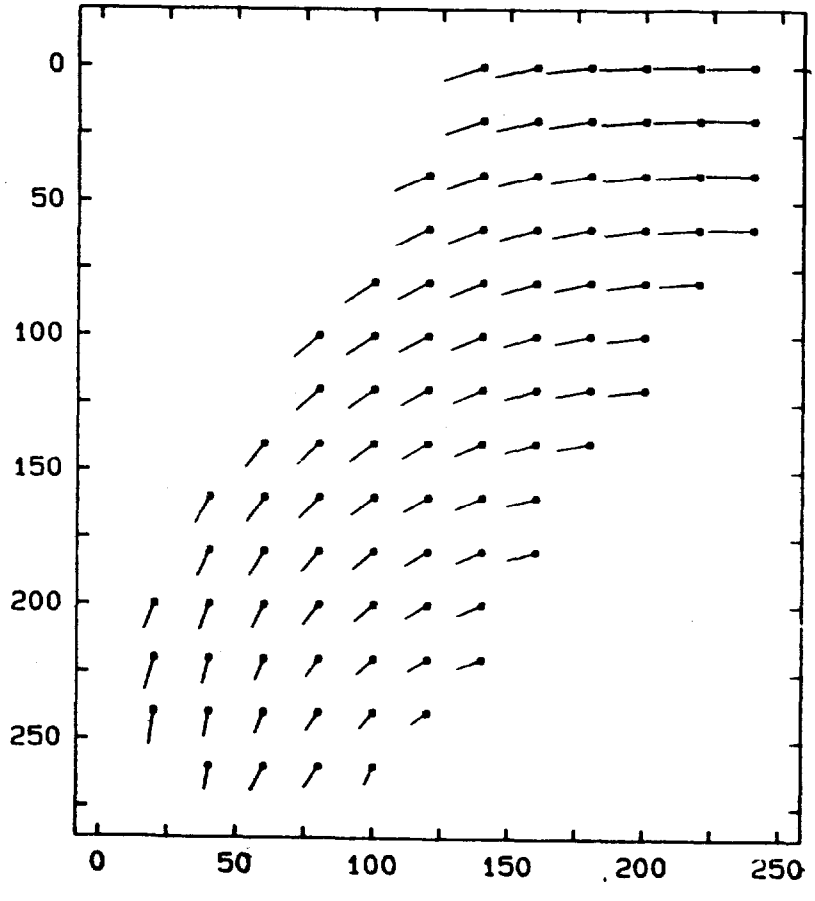

Figure 3. Resulting vector field for LWR 10605, describing the geometric transformation on a regular 20 pixels grid. The axes are denoted with pixel positions in the flat field subimage.

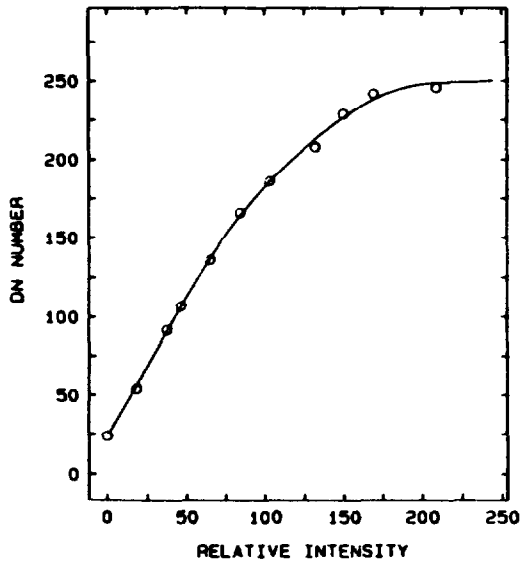

Figure 4. An example of an ITF curve for a single pixel. The circles mark the flat field exposure levels, while the curve shows a fit using a cubic spline interpolation.

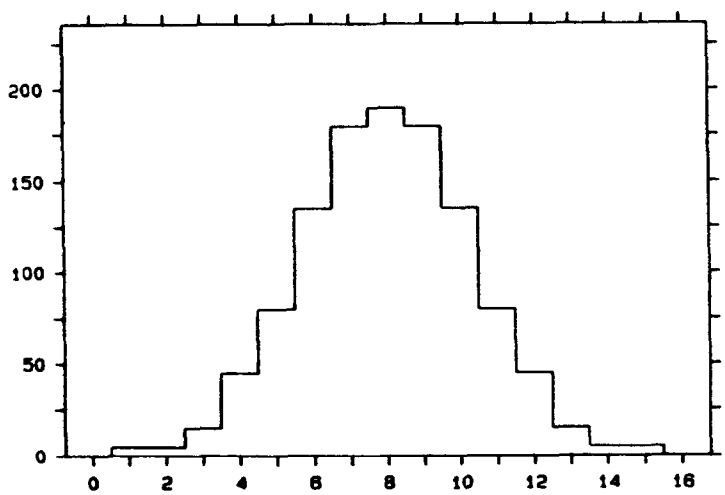

Figure 5. The weighting function for the spectral order containing the Mg II emission lines. The x-axis is denoted with pixel values in the magnified and rotated image. The y-axis represents relative intensity.

6.5 Magnification and rotation

As a preparatory step for the spectrum extraction, the transformed and calibrated image is rotated to align the spectral orders on a horizontal axis. This greatly facilitates the extraction procedure. To avoid excessive degradation from the necessary pixel remapping, and to provide a suitable sampling interval, the image is magnified a factor two by pixel replication, prior to the rotation. Within the rotation procedure, we further limit the analysed image area to three spectral orders (including backgrounds).

6.6 Spectrum extraction

The spectral extraction is made with an optimised slit. This means that a weighting function (see Figure 5), perpendicular to the spectrum, is used for the slit. This function is derived from averages of tracings perpendicular to the spectral orders.

The extraction begins by locating the positions of the studied spectral order and its immediate neighbours. A special routine studies the spectral intensity above the background perpendicular to the dispersion direction, and decides on a spectrum position by computing a weighted average. This is repeated along the spectral order at regular intervals. Finally, the spectrum position is determined to a fraction of a pixel, using a rather stiff spline interpolation through the calculated points. The adjacent spectral order positions are used to calculate the location of the surrounding background.

The background is then extracted using a wide rectangular slit, which automatically provides a suitable smoothing. The spectral order itself is extracted using a weighted 1*15 pixel slit. The slit closely follows the position of the spectrum. Shifts less than 1 pixel, perpendicular to the spectrum, are accounted for by correspondingly shifting the weighting function.

7. Results

The results so far have been very encouraging. However, it is not straightforward to find a reliable quality estimator of possible improvements. For instance, the extraction algorithm used in IUESIPS is so different that results do not easily compare. We have therefore concentrated on checking any resulting enhancements of the corrected image. This has been done by treating our corrected images and the IUESIPS corrected images exactly the same, i.e. the steps described in sections 6.5 and 6.6 have been carried out identically on both images. Note that this ought to produce some improvements also for the case of the IUESIPS corrected image, compared to standard IUESIPS, due to the enhanced spectrum extraction. A rather reliable indicator is the behaviour of the background.

Figure 6 shows a comparison between background extractions using a (1*1 pixel slit), taken from the exposure LWR 10605. The lower part of the figure shows our extraction, while the upper part shows the extraction from the IUESIPS image. The noise is considerably reduced as a result of our image processing. Figure 7 shows the corresponding spectral extractions.

8. Stability and applicability of the method

Test have shown that the method gives improvements for almost all of our exposures. However, the effects are often less striking than the example in Figure 6. This is due to, for example, presence of normal photon noise. Since various threshold parameters are involved at crucial points in the algorithms, some careful tuning is expected to increase the stability and reliability of the method. We have not applied the method to other types

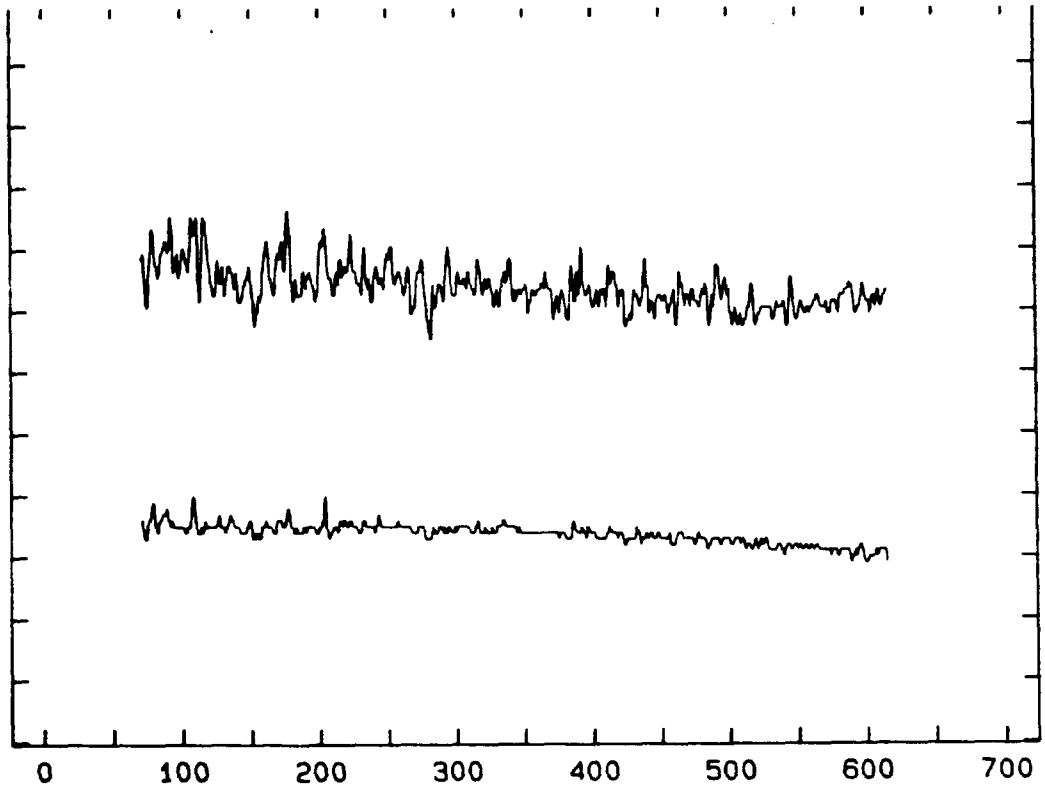

Figure 6. Extracted backgrounds from the LWR 10605 exposure, using a 1*1 pixel slit. The upper extraction is from an IUESIPS corrected image, while the lower extraction is from the Lund corrected image. The x-axis is denoted with pixel numbers in the magnified and rotated image.

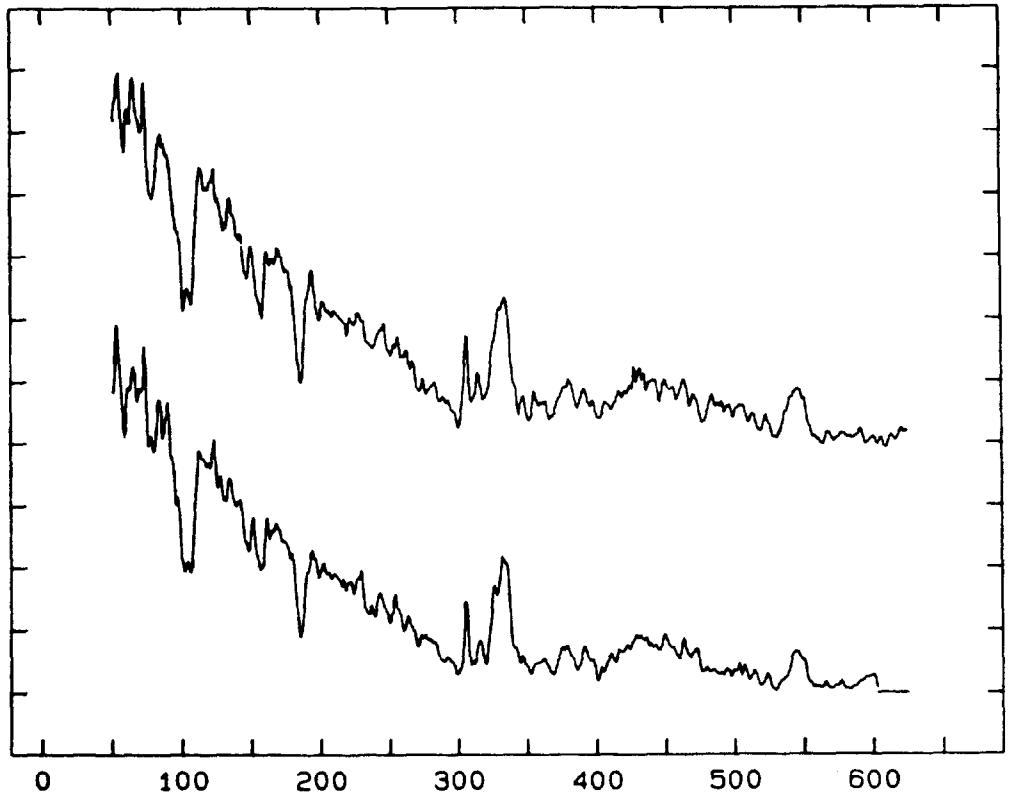

Figure 7. Corresponding spectrum extractions from the LWR 10605 exposure, made with a 1*15 pixels weighted slit. The upper spectrum is from the IUESIPS corrected image while the lower spectrum is from the Lund corrected image. The vertical scale is compressed a factor two, relative to Figure 6. The x-axis is denoted with pixel numbers in the magnified and rotated image. No ripple correction has been made in either case.

of IUE images or to other similar detectors. However, we feel the method should be possible to generalise also to other conditions. The inherent simplicity should allow its application to most IUE images and possibly to detectors like the Faint Object Camera of the Hubble Space Telescope.

In the above we have given an outline of the Lund Observatory method for IUE spectral image processing. The work is still in progress and a more detailed description is to be published elsewhere. A 30 minute video movie has been produced, depicting the various reduction steps outlined above, and including blinking of images, appearance of flat fields, etc. The authors may be contacted for further information on the availability of this VHS video cassette, recorded in the PAL colour system.

This work is supported by the Swedish Board for Space Activities.

Reference

Dravins D., Linde P.: 1980, in W. W. Weiss et al., eds: *IUE Data Reduction*, Wien, p.85

Reprinted from ESA Newsletter No. 29, p.9, January, 1988.

Note added in proof: Recent investigations confirm that results similar to the spectrum shown in Figure 7 can be obtained from exposures taken during the entire IUE lifespan.